Frontiers of Physics
https://doi.org/10.1007/s11467-020-0971-7
Front. Phys.
15(6), 62501 (2020)

RESEARCH ARTICLE

Entangled chimeras in nonlocally coupled bicomponent phase oscillators: From synchronous to asynchronous chimeras

Qiong-Lin Dai[1], Xiao-Xuan Liu[1], Kai Yang[1], Hong-Yan Cheng[1], Hai-Hong Li[1], Fagen Xie[2,†], Jun-Zhong Yang[1,‡]

[1] *School of Science, Beijing University of Posts and Telecommunications, Beijing 100876, China*
[2] *Department of Research and Evaluation, Kaiser Permanente Southern California, Pasadena, CA 91101, USA*
Corresponding authors. E-maill: †xiefagen@yahoo.com, ‡jzyang@bupt.edu.cn
Received October 10, 2019; accepted May 20, 2020

Chimera states, a symmetry-breaking spatiotemporal pattern in nonlocally coupled identical dynamical units, have been identified in various systems and generalized to coupled nonidentical oscillators. It has been shown that strong heterogeneity in the frequencies of nonidentical oscillators might be harmful to chimera states. In this work, we consider a ring of nonlocally coupled bicomponent phase oscillators in which two types of oscillators are randomly distributed along the ring: some oscillators with natural frequency ω_1 and others with ω_2. In this model, the heterogeneity in frequency is measured by frequency mismatch $|\omega_1-\omega_2|$ between the oscillators in these two subpopulations. We report that the nonlocally coupled bicomponent phase oscillators allow for chimera states no matter how large the frequency mismatch is. The bicomponent oscillators are composed of two chimera states, one supported by oscillators with natural frequency ω_1 and the other by oscillators with natural frequency ω_2. The two chimera states in two subpopulations are synchronized at weak frequency mismatch, in which the coherent oscillators in them share similar mean phase velocity, and are desynchronized at large frequency mismatch, in which the coherent oscillators in different subpopulations have distinct mean phase velocities. The synchronization–desynchronization transition between chimera states in these two subpopulations is observed with the increase in the frequency mismatch. The observed phenomena are theoretically analyzed by passing to the continuum limit and using the Ott-Antonsen approach.

Keywords chimera states, bicomponent phase oscillators, nonlocal coupling, desynchronization transition

1 Introduction

In the past decade, we have witnessed a rapid expansion in the study of chimera states as they evolve from a surprising symmetry-breaking spatiotemporal pattern to a prevailing dynamical phenomenon, which ranges from physics and chemistry to biology and from classical to quantum systems [1–16]. Chimera states, characterized by the alternation between coherent and incoherent regions, were originally found numerically by Kuramoto and Battogtokh in 2002 [1] in nonlocally coupled identical phase oscillators and theoretically investigated by Abrams and Strogatz in 2004 [2]. Later, chimera states have been numerically observed in periodic and chaotic maps [17], mechanical oscillators [18], neuronal oscillators [19–21], and chemical oscillators [22]. Since 2012, chimera states have been experimentally demonstrated in mechanical systems [7], chemical systems [8], and optical systems [9]. Different type of chimera states such as breathing chimera states [2], amplitude-mediated chimeras [23], multi-cluster chimeras [5, 24], and spiral chimeras [25–27] have been identified and investigated. Furthermore, chimera states in nonlocally coupled moving phase oscillators have also been studied [28]. Two factors are assumed to be required for chimera states: self-oscillating units and nonlocal coupling. However, the two requirements have been de-emphasized recently. Chimera states have been found in globally coupled oscillators [29–32] as well as in locally coupled oscillators [33, 34]. Moreover, chimera states are found in nonlocally coupled excitable systems. The excitable systems, ubiquitous in biological, chemical, and physical systems, allow for a stable equilibrium and, in response to strong perturbation, they return to equilibrium only after a large excursion. Semenova *et al.* have studied chimera states in nonlocally coupled excitable systems in the presence of noise [35]. Dai *et al.* found that chimera states emerge out of excitable units through a coupling-induced collective oscillation [36]. The relevance of chimera states to other dynamical phenomena has been investigated recently. Motter *et al.* proposed a connection between chimera states and cluster

*arXiv: 1808.03220.

synchronization in networks of locally coupled chaotic oscillators [37]. Lai *et al.* established a connection between chimera states and a quantum scattering phenomenon in two-dimensional Dirac material systems where manifestations of classically integrable and chaotic dynamics simultaneously coexist [12].

Most of the works on chimera states focus on coupled identical oscillators. However, it is very unlikely that real systems such as neuronal systems can be modeled as coupled identical units. The resistance of chimera states to heterogeneity in oscillators is naturally of interest. Laing investigated the problem in the presence of heterogeneity in the intrinsic frequencies of oscillators [3], for example, the natural frequencies of oscillators follow a Lorentzian model with the width measuring the heterogeneity in frequency. For a ring of nonlocally coupled phase oscillators, Laing found that chimera states will be destroyed by strong frequency heterogeneity (large width), although they are resistant to weak frequency heterogeneity (small width) [3]. In his work, Laing focused on the unimodal frequency distribution, where coherent oscillators in a realized chimera state share a similar mean phase velocity. Investigations on synchronization in globally coupled phase oscillators with bimodal frequency distribution revealed that a synchronous state could be a standing wave state where coherent oscillators are partitioned into two coherent clusters with different mean phase velocities [38]. However, one question naturally arises, do chimera states in a ring of nonlocally coupled phase oscillators with bimodal frequency distribution exist and what do they look like? In this work, we study a simple case where the bimodal frequency distribution is modeled by a double-δ distribution. In other words, we study a ring of bicomponent phase oscillators where oscillators are partitioned into two subpopulations. Oscillators in each subpopulation have the same natural frequency, and the natural frequencies of oscillators in different subpopulations are distinct. Another implication exists in the coupled bicomponent oscillators, as the model represents a simple system with heterogeneity in frequency. In the coupled bicomponent phase oscillators, heterogeneity in frequency is measured by frequency mismatch between two subpopulations. It will be interesting to investigate how the existence of chimera states depends on the frequency mismatch between the two subpopulations.

Recently, the interaction between chimera states has been investigated in the form of chimera states in multilayer networks. Ghosh *et al.* considered a two-layer network of chaotic maps with delayed interactions. In their model, chaotic maps in the same layer are nonlocally coupled and inter-layer interaction is mediated by one-to-one coupling between the mirror maps on different layers [39]. They found that the delay and multiplexing collectively produce an improved or suppressed appearance of the chimera state. Maksimenkon *et al.* studied a two-layer network of coupled phase oscillators in which phase oscillators are coupled nonlocally in each layer, and each oscillator in one layer is globally coupled to the other layer [40]. They discovered synchronous and asynchronous chimera states. Chimera states on bipartite network of phase oscillators and Fitzhugh–Nagumo oscillators have been investigated [41, 42], where the interaction between chimera states induces different types of chimera states such as in-phase chimera states, anti-phase chimera states, and syn–desyn chimera states. In these works, at least two layers are required for the underlying network, and each layer supports its own chimera state. Thus, we are interested to see different chimera states coexisting in a single layer. If we can find them, it means that a novel platform can be determined to investigate the interaction between chimera states. Fortunately, this work shows that a ring of nonlocally coupled bicomponent oscillators may act as such a platform.

The rest of the paper is organized as follows: In Section 2, we present the model of nonlocally coupled bicomponent phase oscillators in a ring and provide a brief summary on chimera states in a ring of identical phase oscillators. In Section 3, we demonstrate the existence of chimera states in the bicomponent phase oscillators and a synchronization–desynchronization transition induced by the frequency mismatch among oscillators. We also present a theoretical analysis of the observed chimera states in this section. Finally, we conclude with a summary in Section 4.

2 Model

We consider a ring of coupled phase oscillators, which is described as

$$\dot{\theta}_i(t) = \omega_i - \sum_{j=1}^{N} G(|i-j|)\sin[\theta_i(t) - \theta_j(t) + \alpha]. \tag{1}$$

The subscript i represents the node index, which must be taken modulo N (or period boundary condition). θ_i and ω_i represent the phase and the natural frequency of the oscillator i, respectively. α is the phase lag. The kernel function $G(|i-j|)$ describes how oscillators i and j interact with each other. When $G(|i-j|)$ takes a constant, the model (1) reduces to the well-known Kuramoto model, which is the paradigm model on synchronization in globally coupled nonidentical oscillators [43, 44]. For $G(|i-j|)$ depending on $i-j$, the original Kuramoto model is generalized to the one with nonlocal coupling. Here, we assume the kernel function $G(|i-j|)$ to be even, nonnegative, decreasing with $|i-j|$ and normalized to have unit summation. Defining position-dependent complex order parameters $Z_i = R_i e^{i\Theta_i} = \sum_{j=1}^{N} G(|i-j|)e^{i\theta_j}$, Eq. (1) is reformulated as

$$\dot{\phi}_i = \omega_i - \dot{\Theta}_i - R_i \sin(\phi_i + \alpha) \tag{2}$$

by letting $\phi_i = \theta_i - \Theta_i$. When $|\omega_i - \dot{\Theta}_i| < R_i$, oscillator i

is trapped by the order parameter Z_i.

For kernel function $G(x) = [1 + A\cos(2\pi x/N)]/(2\pi)$ with $0 \leq A \leq 1$ and identical phase oscillators with $\omega_i = \omega$, model (1) becomes the standard model exploring chimera states that allow for chimera states at proper A and α [2]. Previous studies have shown some common features of chimera states in coupled identical oscillators with sufficiently large N as following: $\dot{\Theta}_i$ is independent of position and oscillators satisfying $|\omega - \dot{\Theta}_i| < R_i$ are coherent and frequency-locked to Θ_i.

When the heterogeneity in the natural frequency is introduced, for example, the natural frequencies of oscillators follow a Lorentzian model with nonzero width, Laing found that chimera states are robust as the heterogeneity in frequency is weak (small width) [3]. Here, we are interested in the nonlocally coupled nonidentical phase oscillators with bimodal frequency distribution. We consider the simplest situation, which is the bicomponent phase oscillators, by assuming that the frequency distribution follows a double-δ function $g(\omega) = p\delta(\omega - \omega_1) + (1-p)\delta(\omega - \omega_2)$ with $p \in (0,1)$ and $\omega_1 \geq \omega_2$. Every oscillator is assigned with ω_1 with the probability p, and ω_2 with the probability $1-p$. However, it is the difference $\omega_1 - \omega_2$ that is the relevant parameter and not the sum $\omega_1 + \omega_2$, which can be demonstrated by introducing a new phase variable θ' such that $\dot{\theta}'_i = \dot{\theta}_i - (\omega_1 + \omega_2)/2$. Using the new phase variable θ', the frequency distribution becomes $g(\omega) = p\delta(\omega-\omega_0)+(1-p)\delta(\omega+\omega_0)$ with $\omega_0 = (\omega_1-\omega_2)/2$. Therefore, to reduce the number of controlling parameters, we investigate the model (1) by assuming $\omega_1 = \omega_0$ and $\omega_2 = -\omega_0$. In other words, we study the model (1) in the frame rotating at the frequency $(\omega_1 + \omega_2)/2$. For convenience, we call oscillators with the natural frequency ω_0 positive oscillators and oscillators with $-\omega_0$ negative oscillators. In this bimodal frequency distribution, the heterogeneity in the natural frequency is measured by ω_0, and large ω_0 defined strong heterogeneity in natural frequencies of oscillators. We are interested in how the heterogeneity impacts on chimera dynamics. For example, how does the existence of chimera state in a ring of nonlocally coupled bicomponent phase oscillators depend on ω_0. A pair of phase oscillators display synchronization or desynchronization depending on the frequency mismatch between them. It is also already known in the Kuramoto model with bimodal frequency distribution that partial synchronous states exist with single coherent cluster or two coherent clusters depending on the gap between the peak frequencies. We are interested in whether similar phenomena occur with chimera dynamics in a ring of nonlocally coupled bicomponent phase oscillators.

3 Results

We start with $p = 0.5$, $A = 1$ and $\alpha = 1.45$ and numerically simulate Eq. (1) using a fourth-order Runge–Kutta algorithm with $\delta t = 0.025$. The number of oscillators is $N = 256$. Initially, each oscillator randomly takes its phase in the range of $[0, 2\pi]$. We have checked that the observed results in this work are robust to initial conditions.

Chimera states can exist in a ring of nonlocally coupled bicomponent phase oscillators no matter how strong the heterogeneity in frequencies of oscillators. To show this, we consider $\omega_0 = 0.03$ (weak heterogeneity) and $\omega_0 = 3$ (strong heterogeneity). The top row in Fig. 1 shows the snapshots of oscillators for $\omega_0 = 0.03$ and $\omega_0 = 3$. The snapshots show that oscillators as a whole display one small coherent cluster for $\omega_0 = 0.03$, although no coherent cluster is observed for $\omega_0 = 3$. However, if we treat positive and negative oscillators separately, we find that each subpopulation supports its own chimera state. At $\omega = 0.03$, the coherent cluster in positive oscillators (the black dots) is smaller than that in negative oscillators (the red dots), and the two coherent clusters are overlapped in space. At $\omega_0 = 3$, the coherent clusters in positive and negative oscillators are not overlapped, which prevents the chimera states from being identified from the snapshots of oscillators if positive and negative oscillators are not distinguished. Figures 1(b) and (c) show two types of chimera states at $\omega_0 = 3$. That is, chimera dynamics in positive oscillators are characterized by a chimera state with one coherent cluster in Fig. 1(b) and chimera state with two coherent clusters in Fig. 1(c), whereas only one coherent cluster exists in negative oscillators. Particularly, chimera states can be observed at $\omega_0 = 3$, where positive oscillators comprise one coherent cluster, but negative oscillators possess one or two coherent clusters. In nonlocally coupled single-component phase oscillators, a two-cluster chimera state coexists with a one-cluster chimera state in a large region in the parameter plane of A and α [5]. Hence, the coexistence between chimera states with one or two coherent clusters in positive or negative oscillators evidenced in Figs. 1 (b) and (c) can be observed in a large parameter region in A and α plane at $\omega_0 = 3$. The existence of chimera states at strong heterogeneity in frequencies of oscillators can be understood by taking ω_0 sufficiently large. Letting $\theta_i^{\pm} = \phi_i^{\pm} \pm \omega_0$ for $i \in S_{\pm}$ with $\pm$ representing positive and negative oscillators and $S_{\pm}$ the set of positive and negative oscillators, the model (1) can be reformulated as

$$\dot{\phi}_i^{\pm}(t) = -\sum_{j\in S_{\pm}} G(|i-j|)\sin[\phi_i^{\pm}(t) - \phi_j^{\pm}(t) + \alpha] - \sum_{j\in S_{\mp}} G(|i-j|)\sin[\phi_i^{\pm}(t) - \phi_j^{\mp}(t) \pm 2\omega_0 t + \alpha]. \quad (3)$$

When ω_0 becomes sufficiently large, the last term in Eq. (3) becomes irrelevant to the dynamics of positive and negative oscillators since it changes with time at an extremely fast rate and can be ignored. However, the model (1) decouples to two independent systems that consist of only positive or negative oscillators at sufficiently large ω_0. Consequently, positive and negative oscillators

support specified chimera states, and the chimera states in them are uncorrelated.

The mean phase velocity of an oscillator, defined as $\omega_{e,i} = \langle \dot{\theta}_i \rangle$ with $\langle \cdot \rangle$ the time average over a long time interval, is often used to distinguish the coherent and incoherent oscillators in chimera states. The profiles of $\omega_{e,i}$ in the second row in Fig. 1 show that positive and negative oscillators condensate onto two different curves. At $\omega_0 = 0.03$, the two curves share the same mean phase velocity for coherent oscillators and the mean phase velocities for the coherent clusters in positive and negative oscillators are significantly separated at $\omega_0 = 3$. Moreover, we monitor the spatially-dependent complex order parameter Z_i. $\langle \dot{\Theta}_i \rangle$ and $\langle R_i \rangle$ averaged over a long time interval are presented in the bottom row in Fig. 1. $\langle \dot{\Theta}_i \rangle$ is independent of space at $\omega_0 = 0.03$, whereas it becomes position-dependent at $\omega_0 = 3$. Particularly, in the chimera state with one coherent cluster in positive oscillators at $\omega_0 = 3$, the variance in $\langle \dot{\Theta}_i \rangle$ ranging from -3.4 to 0.5 is stronger. Furthermore, the bottom row in Fig. 1 suggests that the criteria $|\omega_i - \langle \dot{\Theta}_i \rangle| < \langle R_i \rangle$ fails to determine whether an oscillator is in coherent clusters for $\omega_0 = 3$.

The chimera dynamics in the bicomponent phase oscillators can be understood as follows: Bearing in mind that positive and negative oscillators support specified chimera states, we introduce complex order parameters for positive and negative oscillators, respectively,

$$Z_{\pm,i} = R_{\pm,i} e^{i\Theta_{\pm,i}} = \sum_{j \in S_\pm} G(|i-j|) e^{i\theta_{\pm,j}}. \tag{4}$$

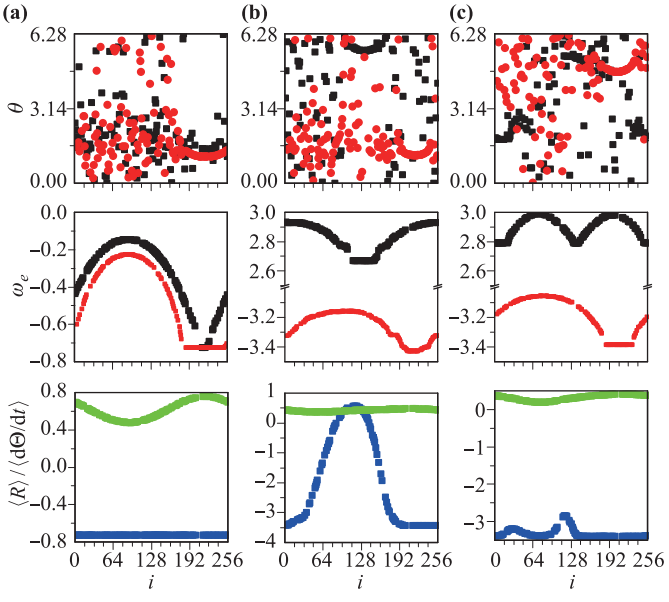

Fig. 1 The chimera states at ω_0=0.03 **(a)**, ω_0=3 **(b)** and **(c)**. The top row shows the snapshots of θ for negative oscillators (red) and positive oscillators (black). The second row shows the mean phase velocities ω_e which condensates onto two curves in corresponding with negative oscillators (red) and positive oscillators (black). The third row shows $\langle R \rangle$ (green) and $\langle d\Theta/dt \rangle$ (blue). $A = 1$ and $\alpha = 1.45$.

Then Eq. (1) is reformulated as

$$\begin{aligned} \dot{\phi}_{\pm,i} = &\pm \omega_0 - \dot{\Theta}_{\pm,i} - R_{\pm,i} \sin(\phi_{\pm,i} + \alpha) \\ &- R_{\mp,i} \sin(\phi_{\pm,i} + \Theta_{\pm,i} - \Theta_{\mp,i} + \alpha) \end{aligned} \tag{5}$$

with $\phi_{\pm,i} = \theta_{\pm,i} - \Theta_{\pm,i}$. Defining the quantity $\Delta\Omega_{\pm,i}$ as

$$\begin{aligned} \Delta\Omega_{\pm,i} = &\pm \omega_0 - \dot{\Theta}_{\pm,i} \\ &- R_{\mp,i} \sin(\phi_{\pm,i} + \Theta_{\pm,i} - \Theta_{\mp,i} + \alpha), \end{aligned} \tag{6}$$

we conjecture that positive and negative oscillators will get trapped by $Z_\pm$, respectively, if they satisfy the condition $|\langle \Delta\Omega_{\pm,i} \rangle| < \langle R_{\pm,i} \rangle$. In Fig. 2, the positive and negative oscillators are plotted separately. From the middle row, we find that $\langle \dot{\Theta}_{\pm,i} \rangle$ are in coincidence with the mean phase velocities of coherent positive and negative oscillators, respectively. The bottom row in Fig. 2 shows that $|\langle \Delta\Omega_{\pm,i} \rangle| < \langle R_{\pm,i} \rangle$ is satisfied only in coherent clusters, which demonstrates the validity of the description based on Eqs. (4)–(6).

There is one extraordinary feature in Fig. 2, $\langle \dot{\Theta}_{+,i} \rangle = \langle \dot{\Theta}_{-,i} \rangle$ at $\omega_0 = 0.03$, whereas the equality is broken at $\omega_0 = 3$. The feature reveals synchronization between the chimera dynamics in positive and negative oscillators at $\omega_0 = 0.03$ and desynchronization between these two chimera dynamics at $\omega_0 = 3$. We term the former states as synchronous chimera states and the latter as asynchronous chimera states. $\langle \dot{\Theta}_{\pm,i} \rangle$ remains constant in the synchronous chimera states but displays a level of inhomogeneity in space in the asynchronous chimera states. Consequently, chimera dynamics in a ring of bicomponent phase oscillators may display both synchronous and asynchronous chimera states, depending on the parameter ω_0. Furthermore, the position-dependence of $\langle \dot{\Theta}_i \rangle$ can be heuristically explained as follows: Since $Z_i = Z_{+,i} + Z_{-,i}$, supposing R_i and $R_{\pm,i}$ to be time-independent for simplicity, we have

$$\dot{\Theta}_i = \frac{R_{+,i}}{R_i} \cos(\Theta_{+,i} - \Theta_i) \dot{\Theta}_{+,i} + \frac{R_{-,i}}{R_i} \cos(\Theta_{-,i} - \Theta_i) \dot{\Theta}_{-,i}.$$

$\dot{\Theta}_{\pm,i}$ and $R_{\pm,i}/R_i$ contribute to the position-dependence of $\dot{\Theta}_i$. Therefore, both $\langle \dot{\Theta}_{+,i} \rangle \neq \langle \dot{\Theta}_{-,i} \rangle$ and the mismatch of the coherent clusters in positive and negative oscillators in space for $\omega_0 = 3$ shown in Fig. 2 lead to the position dependence of $\dot{\Theta}_i$.

We can discuss the chimera dynamics in bicomponent phase oscillators in another way. Consider that either positive oscillators (for example, $p = 1$) or negative oscillators (for example, $p = 0$) can support chimera state in which the mean phase velocity of the coherent oscillators is determined by ω_0 or $-\omega_0$. That is, ω_0 measures the frequency mismatch between the coherent oscillators in chimera states in positive oscillators ($p = 1$) and negative oscillators ($p = 0$). Once p is between 0 and 1, the frequency mismatch measured by ω_0 determines whether the chimera state in bicomponent phase oscillators is synchronous or asynchronous. Realized synchronous chimera

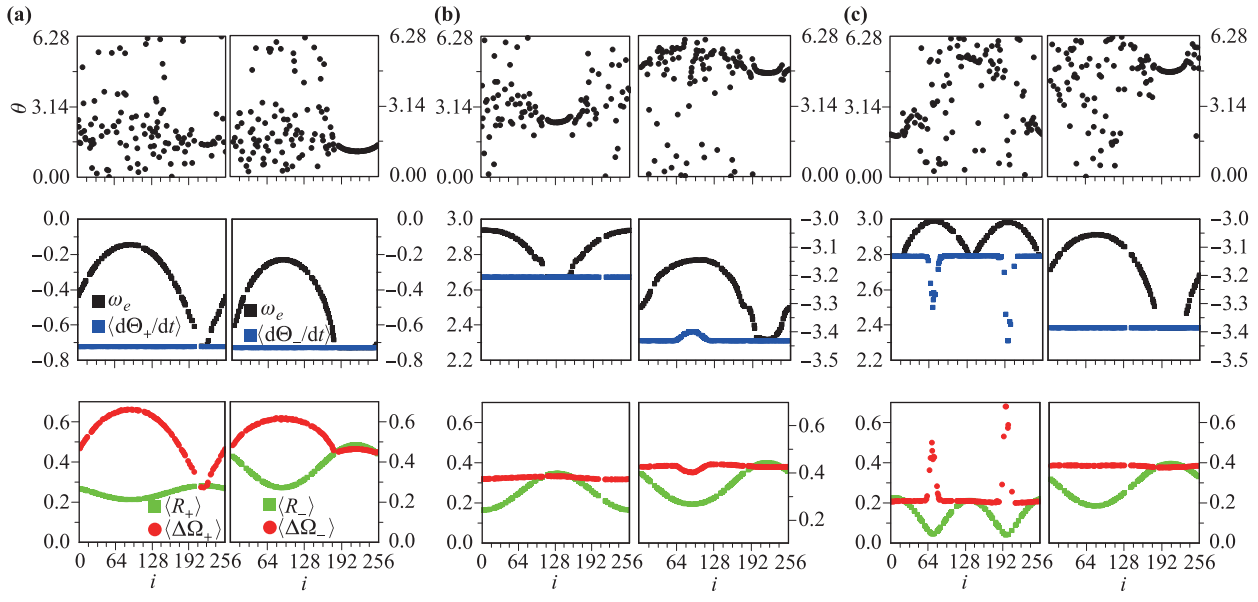

Fig. 2 The chimera states at $\omega_0 = 0.03$ **(a)**, $\omega_0 = 3$ **(b)** and **(c)**. In each plot, the left column shows the results for positive oscillators and the right column for negative oscillators. The top row shows the snapshots of θ, the middle row shows ω_e (black) and $\langle \mathrm{d}\Theta_\pm/\mathrm{d}t\rangle$ (blue), and the bottom row shows $\langle R_\pm\rangle$ (green) and $\langle \Delta\Omega_\pm\rangle$ (red). $A = 1$ and $\alpha = 1.45$.

state at $\omega_0 = 0.03$ and asynchronous chimera state at $\omega_0 = 3$ in bicomponent phase oscillators are simply the results due to the interplay between chimera states in the positive and negative oscillators.

The transition between the synchronous and asynchronous chimera states can be investigated by monitoring $\langle \dot{\Theta}_{\pm,i}\rangle$ against ω_0. Since $\langle \dot{\Theta}_{+,i}\rangle$ exhibits strong inhomogeneity in asynchronous chimera states with two coherent clusters, we also record its maximum and minimum with the variance of the node index for each ω_0. Numerical simulations show that the mean phase velocity of coherent positive oscillators is represented by the maximum of $\langle \dot{\Theta}_{+,i}\rangle$. Figure 3 shows that the transition occurs at approximately $\omega_{0c} = 0.12$ where the maximum of $\langle \dot{\Theta}_{+,i}\rangle$ departs from $\langle \dot{\Theta}_{-,i}\rangle$. Before ω_{0c}, $\langle \dot{\Theta}_{\pm,i}\rangle$ is a constant and $\langle \dot{\Theta}_{+,i}\rangle = \langle \dot{\Theta}_{-,i}\rangle$ is held, which suggests that chimera states in positive and negative oscillators get synchronized, which yields a synchronous chimera state in bicomponent phase oscillators. Beyond ω_{0c}, the asynchronous chimera state with two coherent clusters first appears and, next, the asynchronous chimera state with one coherent cluster is observed at approximately $\omega_0 = 0.4$. The inset in Fig. 3 shows the transition at other combination of A and α, where $\langle \dot{\Theta}_{-,i}\rangle$ and the maximum of $\langle \dot{\Theta}_{+,i}\rangle$ are plotted, which supports the transition between synchronous and asynchronous chimera states for positive and negative oscillators is unexceptional. In summary, a synchronization–desynchronization transition with ω_0 between two chimera dynamics simultaneously existing in the same population, which is an interesting observation in the field of chimera states, is shown in Fig. 3.

The existence of chimera states in identical phase oscillators depends on the parameters A and α. We are interested in how robust the synchronous chimera states and asynchronous chimera states are to the variation of parameters A and α in bicomponent phase oscillators. We focus on synchronous chimera states at $\omega_0 = 0.06$ and asynchronous chimera states at $\omega_0 = 3$. For convenience, we will not distinguish the asynchronous chimera states with two coherent clusters and those with one coherent cluster. To obtain the boundary of the stability diagram for these chimera states, we consider two paths by continu-

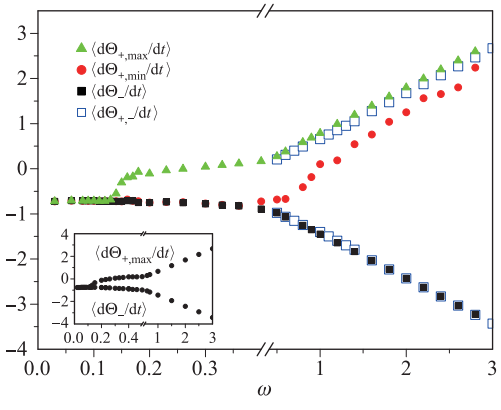

Fig. 3 The desynchronization transition from synchronous chimera states to asynchronous chimera states at $A = 1$ and $\alpha = 1.45$. The solid symbols are acquired from synchronous chimera states and asynchronous chimera states with two coherent clusters in positive oscillators and the open symbols are from the asynchronous chimera states with one coherent clusters in positive oscillators. The inset shows another example at $A = 0.89$ and $\alpha = 1.38$.

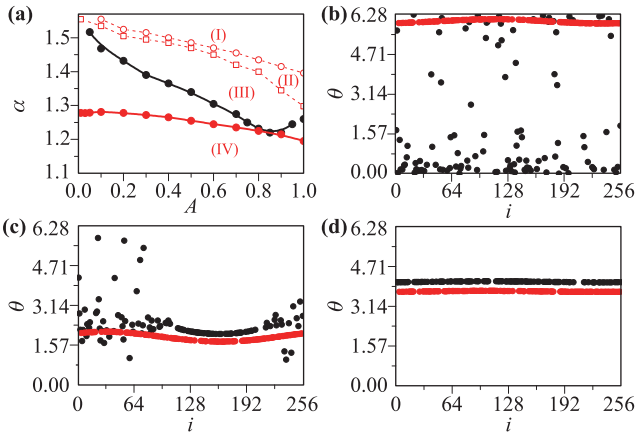

Fig. 4 **(a)** The stability diagrams in the plane of A and α of synchronous chimera states at $\omega_0 = 0.06$ (red) and asynchronous chimera states at $\omega_0 = 3$ (black). The open symbols with dashed line further divide the parameter plane into four regimes at $\omega_0 = 0.06$, for example, incoherent-chimera state with incoherence for positive oscillators and chimera state for negative oscillators in the regime (I), incoherent-coherent state in the regime (II), incoherent-chimera state in the regime (III), and coherent-coherent state in the regime (IV). **(b–d)** The dynamical states represented by the snapshots θ at $\alpha = 1.31$ in the regime (II), $\alpha = 1.24$ in the regime (III), and $\alpha = 1.1$ in the regime (IV) show the transition scenario from synchronous chimera states to synchronous states at $\omega_0 = 0.06$ and $A = 1$.

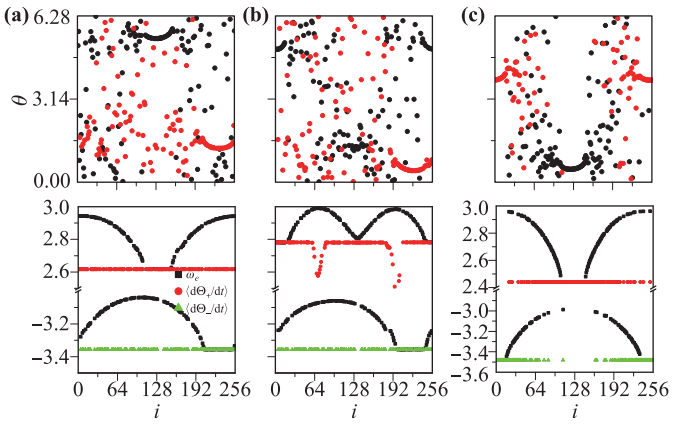

Fig. 5 **(a, b)** Chimera states with one coherent cluster in positive oscillators and with two coherent clusters in positive oscillators at $p = 0.6$. **(c)** Chimera states with one coherent cluster in positive oscillators with $p(i) = \sin(\pi i/N)$. The top panels show the snapshots for positive oscillators (black) and negative oscillators (red). The bottom panels show the mean phase velocity (black), $\langle\dot{\Theta}_{+,i}\rangle$ (red) and $\langle\dot{\Theta}_{-,i}\rangle$ (green). $A = 1$, $\alpha = 1.45$, and $\omega_0 = 3$.

ously decreasing A with fixed α and continuously decreasing α with fixed A. The stability diagrams are presented in Fig. 4(a). We find that the critical α tends to increase with the decrease of A for both types of chimera states, and the parameter regime for synchronous chimera states is considerably larger than that for asynchronous chimera states. Comparing with the stability diagram of chimera state in nonlocally coupled identical phase oscillators [2], a ring of bicomponent phase oscillators supports chimera states in significantly larger parameter regimes. Figures 4(b)-(d) show a transition scenario at $\omega_0 = 0.06$ and $A = 1$. With α decrease, positive oscillators first transit to incoherence and back to chimera dynamics and finally to an all-coherent state. However, chimera dynamics in negative oscillators are replaced by all-coherent dynamics with α decrease. Combining these results together, we can determine incoherent-chimera state, incoherent-coherent state [Fig. 4(b)], chimera-coherent state [Fig. 4(c)], and coherent-coherent state [Fig. 4(d)]. The critical curves separating these states from each other at $\omega_0 = 0.06$ are shown in Fig. 4(a).

The parameter p accounts for a fraction of positive oscillators in the population of phase oscillators. The qualitative properties of the model dynamics in bicomponent phase oscillators are not sensitive to p. Figures 5(a) and (b) show an example at $p = 0.6$, where asynchronous chimera states with one coherent cluster and two coherent clusters at $\omega_0 = 3$ are presented, respectively. Moreover, the model dynamics remain unchanged even when p is position-dependent. Figure 5(c) shows the asynchronous chimera states with one-coherent cluster at $\omega_0 = 3$ for $p(i) = \sin(\pi i/N), i = 1, 2, \cdots, N$.

The ring of nonlocally coupled bicomponent phase oscillators, when the number of phase oscillators approaches infinity, can be analyzed using the Ott–Antonsen ansatz [3, 45]. The length of the ring is set to be 2π. We consider the probability density function $f_\pm(x, \theta, t)$ defined as the fraction of positive/negative oscillators with phases between θ and $\theta + \mathrm{d}\theta$ at time t and position x, respectively. The two functions satisfy the continuity equations

$$\frac{\partial f_\pm}{\partial t} + \frac{\partial (f_\pm v_\pm)}{\partial \theta} = 0. \tag{7}$$

Reformulating the order parameters for positive and negative oscillators

$$Z_\pm(x) = \int_0^{2\pi} G(x - x') \int_0^{2\pi} \mathrm{e}^{\mathrm{i}\theta} f_\pm \mathrm{d}\theta \mathrm{d}x', \tag{8}$$

we have

$$v_\pm = \omega_{0,\pm} - \frac{1}{2i}[Z^* \mathrm{e}^{\mathrm{i}(\theta+\alpha)} - Z\mathrm{e}^{-\mathrm{i}(\theta+\alpha)}], \tag{9}$$

where $Z = pZ_+ + (1-p)Z_-$ and Z^* denotes the complex conjugate of Z. Using Ott–Antonsen ansatz, we write the probability density functions as

$$f_\pm(x, \theta, t) = \frac{1}{2\pi}\{1 + \sum_{n=1}^{\infty}[a_\pm^n(x, t)\mathrm{e}^{\mathrm{i}n\theta} + c.c.]\}, \tag{10}$$

where $c.c.$ is the complex conjugate of the previous term. By substituting Eqs. (9) and (10) into Eqs. (7) and (8),

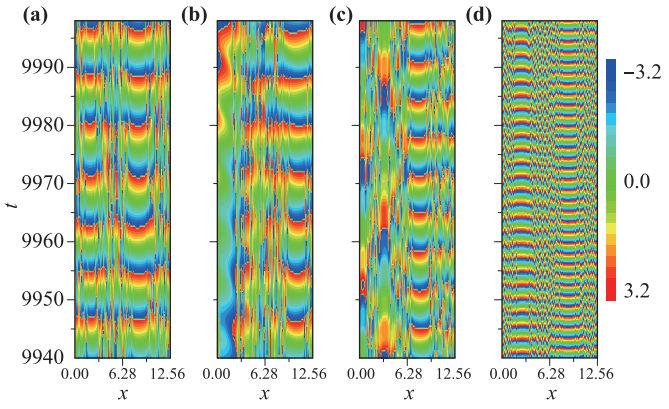

Fig. 6 The evolutions of the arguments of $a_{\pm}$ acquired by simulating Eq. (11) at $\omega_0 = 0.03$ in **(a)**, $\omega_0 = 0.2$ in **(b)**, $\omega_0 = 0.5$ in **(c)**, $\omega_0 = 3$ in **(d)**. For the better illustration, we shift the space variable of a_- from x to $x + 2\pi$. $A = 1$, $\alpha = 1.45$, and $p = 0.5$.

we obtain

$$\frac{\partial a_{\pm}(x,t)}{\partial t} = -\mathrm{i}\omega_{0,\pm} + \frac{1}{2}[Z^*(x,t)\mathrm{e}^{\mathrm{i}\alpha} - Z(x,t)\mathrm{e}^{-\mathrm{i}\alpha}a_{\pm}^2],$$
$$Z(x,t) = \int_0^{2\pi} G(x-x')[pa_+^*(x') + (1-p)a_-^*(x')]\mathrm{d}x'. \tag{11}$$

Numerically simulating Eq. (11), we obtain the evolutions of $a_{\pm}(x,t)$. We present the arguments of $a_{\pm}(x,t)$ in Fig. 6 for several ω_0 by shifting the space variable of $a_-(x,t)$ to $x + 2\pi$. Note that both the position-dependent order parameters and the moduli of $a_{\pm}(x,t)$ are continuous concerning x, but the arguments of $a_{\pm}(x,t)$ are not. Synchronous chimera states at $\omega_0 = 0.03$ and asynchronous chimera states at $\omega_0 = 3$ are reproduced. Particularly, the coherent clusters in a_+ and a_- at $\omega_0 = 3$ overlap in space, which is a little different from the results in Figs. 1 and 2. The discrepancy between Figs. 1, 2, and 6 at $\omega_0 = 3$ is caused by the distribution of positive and negative oscillators on the ring. In Figs. 1 and 2, where a finite number of oscillators are considered, the numbers of positive and negative oscillators in any local environment fluctuate along the ring. However, Eq. (11) is obtained in the limit of an infinite number of oscillators, in which we have assumed the uniform distribution of positive and negative oscillators along the ring. Furthermore, we can obtain the same chimera dynamics in a finite number of phase oscillators at $p = 0.5$, as shown in Fig. 6, with the arrangement of bicomponent oscillators such that positive and negative oscillators alternate along the ring. Following this arrangement, the chimera dynamics obtained from the model Eq. (1) is presented in Fig. 7, which is identical to those in Fig. 6. Moreover, the spatiotemporal patterns in Fig. 6(b) and Fig. 7(b) display a traveling-wave-like behavior for positive oscillators, and we simply present them in a short time span to be consistent with other plots in the figures.

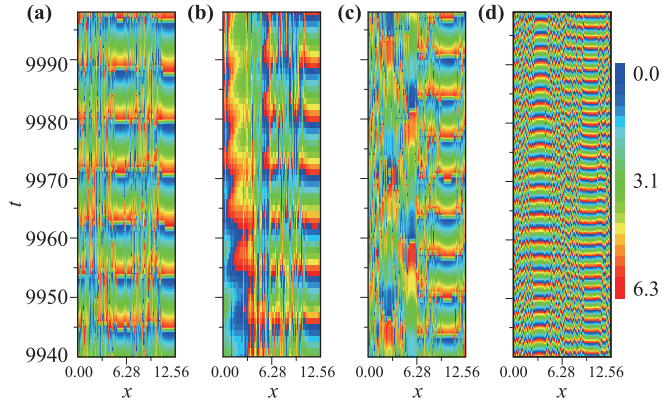

Fig. 7 The evolutions of $\theta_{\pm}$ in Eq. (1) where positive and negative oscillators alternate along the ring at $\omega_0 = 0.03$ in **(a)**, $\omega_0 = 0.2$ in **(b)**, $\omega_0 = 0.5$ in **(c)**, $\omega_0 = 3$ in **(d)**. For the better illustration, we shift the space variable of negative oscillators from x to $x + 2\pi$. $A = 1$, $\alpha = 1.45$, and $p = 0.5$.

4 Conclusion

To conclude, we have studied a ring of nonlocally coupled bicomponent phase oscillators where oscillators are randomly assigned to natural frequency ω_0 and $-\omega_0$. We obtained the existence of chimera states irrespective of how large ω_0 is. Unlike ordinary chimera states in nonlocally coupled identical phase oscillators, the existence of chimera states can be dissimulated if incorrect measurements are taken. By considering both positive and negative oscillators separately, we found that positive and negative oscillators support specified chimera dynamics. Two types of chimera states exist in a ring of bicomponent phase oscillators, synchronous chimera states at small ω_0, where the mean phase velocities in the coherent clusters for positive and negative oscillators are the same, and asynchronous chimera states at large ω_0, where coherent positive and coherent negative oscillators have different mean phase velocities. Increasing ω_0 can induce transition from synchronous to asynchronous chimera states. The existence of synchronous and asynchronous chimera states in nonlocally coupled bicomponent phase oscillators is confirmed by theoretical analysis based on Ott-Antonsen ansatz, which shows exactly similar patterns as those obtained by directly simulating the model (1) with a finite number of phase oscillators. Chimera states are stable only in an infinite number of nonlocally coupled oscillators [46]. However, numerical simulations have suggested that chimera states on a ring are extremely long-lived transient for sufficiently large N [47]. We have tested it for our model with $N = 64$, much less than the system size used in this work, and found that, both synchronous and asynchronous chimera states could survive at least 10^5 time units. Nevertheless, we notice that trimodal fre-

quency distributions in coupled networks have been considered in the previous study [48]. Along this line, chimera states in the network with multi-component frequency distributions as a possible extension to this work can be explored in future research.

Acknowledgements This work was supported by the National Natural Science Foundation of China (Grants Nos. 11575036 and 11805021).

References

1. Y. Kuramoto and D. Battogtokh, Coexistence of coherence and incoherence in nonlocally coupled phase oscillators, *Nonlinear Phenom. Complex Syst.* 5, 380 (2002)
2. D. M. Abrams and S. H. Strogatz, Chimera states for coupled oscillators, *Phys. Rev. Lett.* 93(17), 174102 (2004)
3. C. R. Laing, The dynamics of chimera states in heterogeneous Kuramoto networks, *Physica D* 238(16), 1569 (2009)
4. A. E. Motter, Nonlinear dynamics: Spontaneous synchrony breaking, *Nat. Phys.* 6(3), 164 (2010)
5. Y. Zhu, Y. Li, M. Zhang, and J. Yang, The oscillating two-cluster chimera state in non-locally coupled phase oscillators, *EPL* 97(1), 10009 (2012)
6. M. J. Panaggio and D. M. Abrams, Chimera states: Coexistence of coherence and incoherence in networks of coupled oscillators, *Nonlinearity* 28(3), R67 (2015)
7. E. A. Martens, S. Thutupalli, A. Fourrière, and O. Hallatschek, Chimera states in mechanical oscillator networks, *Proc. Natl. Acad. Sci. USA* 110(26), 10563 (2013)
8. M. R. Tinsley, S. Nkomo, and K. Showalter, Chimera and phasecluster states in populations of coupled chemical oscillators, *Nat. Phys.* 8(9), 662 (2012)
9. A. M. Hagerstrom, T. E. Murphy, R. Roy, P. Hövel, I. Omelchenko, and E. Schöll, Experimental observation of chimeras in coupled-map lattices, *Nat. Phys.* 8(9), 658 (2012)
10. H. Cheng, Q. Dai, N. Wu, Y. Feng, H. Li, and J. Yang, Chimera states in nonlocally coupled phase oscillators with biharmonic interaction, *Commun. Nonlinear Sci. Numer. Simul.* 56, 1 (2018)
11. S. S. Gavrilov, Polariton chimeras: Bose–Einstein condensates with intrinsic chaoticity and spontaneous long range ordering, *Phys. Rev. Lett.* 120(3), 033901 (2018)
12. H. Xu, G. Wang, L. Huang, and Y. Lai, Chaos in Dirac electron optics: Emergence of a relativistic quantum chimera, *Phys. Rev. Lett.* 120(12), 124101 (2018)
13. Z. Wei, F. Parastesh, H. Azarnoush, S. Jafari, D. Ghosh, M. Perc, and M. Slavinec, Nonstationary chimeras in a neuronal network, *EPL* 123(4), 48003 (2018)
14. B. K. Bera, S. Rakshit, D. Ghosh, and J. Kurths, Spike chimera states and firing regularities in neuronal hypernetworks, *Chaos* 29(5), 053115 (2019)
15. S. Rakshit, B. K. Bera, M. Perc, and D. Ghosh, Basin stability for chimera states, *Sci. Rep.* 7(1), 2412 (2017)
16. B. K. Bera, D. Ghosh, and T. Banerjee, Imperfect traveling chimera states induced by local synaptic gradient coupling, *Phys. Rev. E* 94(1), 012215 (2016)
17. I. Omelchenko, Y. Maistrenko, P. Hövel, and E. Schöll, Loss of coherence in dynamical networks: Spatial chaos and chimera states, *Phys. Rev. Lett.* 106(23), 234102 (2011)
18. I. Omelchenko, A. Zakharova, P. Hövel, J. Siebert, and E. Schöll, Nonlinearity of local dynamics promotes multichimeras, *Chaos* 25(8), 083104 (2015)
19. I. Omelchenko, O. E. Omelchenko, P. Hövel, and E. Schöll, When nonlocal coupling between oscillators becomes stronger: Patched synchrony or multichimera states, *Phys. Rev. Lett.* 110(22), 224101 (2013)
20. J. Hizanidis, V. Kanas, A. Bezerianos, and T. Bountis, Chimera states in networks of nonlocally coupled Hindmarsh–Rose neuron models, *Int. J. Bifurcat. Chaos* 24(03), 1450030 (2014)
21. H. Sakaguchi, Instability of synchronized motion in nonlocally coupled neural oscillators, *Phys. Rev. E* 73(3), 031907 (2006)
22. J. F. Totz, J. Rode, M. R. Tinsley, K. Showalter, and H. Engel, Spiral wave chimera states in large populations of coupled chemical oscillators, *Nat. Phys.* 14(3), 282 (2018)
23. A. Zakharova, M. Kapeller, and E. Schöll, Chimera death: Symmetry breaking in dynamical networks, *Phys. Rev. Lett.* 112(15), 154101 (2014)
24. Y. L. Maistrenko, A. Vasylenko, O. Sudakov, R. Levchenko, and V. L. Maistrenko, Cascades of multiheaded chimera states for coupled phase oscillators, *Int. J. Bifurcat. Chaos* 24(08), 1440014 (2014)
25. E. A. Martens, C. R. Laing, and S. H. Strogatz, Solvable model of spiral wave chimeras, *Phys. Rev. Lett.* 104(4), 044101 (2010)
26. C. Gu, G. St-Yves, and J. Davidsen, Spiral wave chimeras in complex oscillatory and chaotic systems, *Phys. Rev. Lett.* 111(13), 134101 (2013)
27. S. Guo, Q. Dai, H. Cheng, H. Li, F. Xie, and J. Yang, Spiral wave chimera in two-dimensional nonlocally coupled Fitzhugh–Nagumo systems, *Chaos Solitons Fractals* 114, 394 (2018)
28. W. Wang, Q. Dai, H. Cheng, H. Li, and J. Yang, Chimera dynamics in nonlocally coupled moving phase oscillators, *Front. Phys.* 14(4), 43605 (2019)
29. A. Yeldesbay, A. Pikovsky, and M. Rosenblum, Chimera-like states in an ensemble of globally coupled oscillators, *Phys. Rev. Lett.* 112(14), 144103 (2014)
30. G. C. Sethia and A. Sen, Chimera states: The existence criteria revisited, *Phys. Rev. Lett.* 112(14), 144101 (2014)
31. V. K. Chandrasekar, R. Gopal, A. Venkatesan, and M. Lakshmanan, Mechanism for intensity-induced chimera states in globally coupled oscillators, *Phys. Rev. E* 90(6), 062913 (2014)

32. K. Premalatha, V. K. Chandrasekar, M. Senthilvelan, and M. Lakshmanan, Impact of symmetry breaking in networks of globally coupled oscillators, *Phys. Rev. E* 91(5), 052915 (2015)
33. C. R. Laing, Chimeras in networks with purely local coupling, *Phys. Rev. E* 92, 050904(R) (2015)
34. B. K. Bera, D. Ghosh, and M. Lakshmanan, Chimera states in bursting neurons, *Phys. Rev. E* 93(1), 012205 (2016)
35. N. Semenova, A. Zakharova, V. Anishchenko, and E. Schöll, Coherence-resonance chimeras in a network of excitable elements, *Phys. Rev. Lett.* 117(1), 014102 (2016)
36. Q. Dai, M. Zhang, H. Cheng, H. Li, F. Xie, and J. Yang, From collective oscillation to chimera state in a nonlocally coupled excitable system, *Nonlinear Dyn.* 91(3), 1723 (2018)
37. Y. S. Cho, T. Nishikawa, and A. E. Motter, Stable chimeras and independently synchronizable clusters, *Phys. Rev. Lett.* 119(8), 084101 (2017)
38. E. A. Martens, E. Barreto, S. H. Strogatz, E. Ott, P. So, and T. M. Antonsen, Exact results for the Kuramoto model with a bimodal frequency distribution, *Phys. Rev. E* 79(2), 026204 (2009)
39. S. Ghosh, A. Kumar, A. Zakharova, and S. Jalan, Birth and death of chimera: Interplay of delay and multiplexing, *EPL* 115(6), 60005 (2016)
40. V. A. Maksimenko, V. V. Makarov, B. K. Bera, D. Ghosh, S. K. Dana, M. V. Goremyko, N. S. Frolov, A. A. Koronovskii, and A. E. Hramov, Excitation and suppression of chimera states by multiplexing, *Phys. Rev. E* 94(5), 052205 (2016)
41. Q. Dai, Q. Liu, H. Cheng, H. Li, and J. Yang, Chimera states in a bipartite network of phase oscillators, *Nonlinear Dyn.* 92(2), 741 (2018)
42. Z. Wu, H. Cheng, Y. Feng, H. Li, Q. Dai, and J. Yang, Chimera states in bipartite networks of FitzHugh–Nagumo oscillators, *Front. Phys.* 13(2), 130503 (2018)
43. Y. Kuramoto, Chemical Oscillations, Waves, and Turbulence, Springer Series in Synergetics, Berlin: Springer-Verlag, 1984
44. J. A. Acebrón, L. L. Bonilla, C. J. Pérez Vicente, F. Ritort, and R. Spigler, The Kuramoto model: A simple paradigm for synchronization phenomena, *Rev. Mod. Phys.* 77(1), 137 (2005)
45. E. Ott and T. M. Antonsen, Low dimensional behavior of large systems of globally coupled oscillators, *Chaos* 18(3), 037113 (2008)
46. O. E. Omel' chenko, Coherence-incoherence patterns in a ring of non-locally coupled phase oscillators, *Nonlinearity* 26(9), 2469 (2013)
47. M. Wolfrum and O. E. Omel' chenko, Chimera states are chaotic transients, *Phys. Rev. E* 84(1), 015201 (2011)
48. B. Pietras, N. Deschle, and A. Daffertshofer, Equivalence of coupled networks and networks with multimodal frequency distributions: Conditions for the bimodal and trimodal case, *Phys. Rev. E* 94, 052211 (2011)